Branching Fractions of τ Leptons to Three Charged Hadrons

R. A. Briere,[1] G. P. Chen,[1] T. Ferguson,[1] G. Tatishvili,[1] H. Vogel,[1] N. E. Adam,[2] J. P. Alexander,[2] K. Berkelman,[2] V. Boisvert,[2] D. G. Cassel,[2] P. S. Drell,[2] J. E. Duboscq,[2] K. M. Ecklund,[2] R. Ehrlich,[2] R. S. Galik,[2] L. Gibbons,[2] B. Gittelman,[2] S. W. Gray,[2] D. L. Hartill,[2] B. K. Heltsley,[2] L. Hsu,[2] C. D. Jones,[2] J. Kandaswamy,[2] D. L. Kreinick,[2] A. Magerkurth,[2] H. Mahlke-Krüger,[2] T. O. Meyer,[2] N. B. Mistry,[2] J. R. Patterson,[2] D. Peterson,[2] J. Pivarski,[2] S. J. Richichi,[2] D. Riley,[2] A. J. Sadoff,[2] H. Schwarthoff,[2] M. R. Shepherd,[2] J. G. Thayer,[2] D. Urner,[2] T. Wilksen,[2] A. Warburton,[2] M. Weinberger,[2] S. B. Athar,[3] P. Avery,[3] L. Breva-Newell,[3] V. Potlia,[3] H. Stoeck,[3] J. Yelton,[3] K. Benslama,[4] B. I. Eisenstein,[4] G. D. Gollin,[4] I. Karliner,[4] N. Lowrey,[4] C. Plager,[4] C. Sedlack,[4] M. Selen,[4] J. J. Thaler,[4] J. Williams,[4] K. W. Edwards,[5] D. Besson,[6] X. Zhao,[6] S. Anderson,[7] V. V. Frolov,[7] D. T. Gong,[7] Y. Kubota,[7] S. Z. Li,[7] R. Poling,[7] A. Smith,[7] C. J. Stepaniak,[7] J. Urheim,[7] Z. Metreveli,[8] K. K. Seth,[8] A. Tomaradze,[8] P. Zweber,[8] S. Ahmed,[9] M. S. Alam,[9] J. Ernst,[9] L. Jian,[9] M. Saleem,[9] F. Wappler,[9] K. Arms,[10] E. Eckhart,[10] K. K. Gan,[10] C. Gwon,[10] K. Honscheid,[10] D. Hufnagel,[10] H. Kagan,[10] R. Kass,[10] T. K. Pedlar,[10] E. von Toerne,[10] M. M. Zoeller,[10] H. Severini,[11] P. Skubic,[11] S. A. Dytman,[12] J. A. Mueller,[12] S. Nam,[12] V. Savinov,[12] J. W. Hinson,[13] J. Lee,[13] D. H. Miller,[13] V. Pavlunin,[13] B. Sanghi,[13] E. I. Shibata,[13] I. P. J. Shipsey,[13] D. Cronin-Hennessy,[14] A. L. Lyon,[14] C. S. Park,[14] W. Park,[14] J. B. Thayer,[14] E. H. Thorndike,[14] T. E. Coan,[15] Y. S. Gao,[15] F. Liu,[15] Y. Maravin,[15] R. Stroynowski,[15] M. Artuso,[16] C. Boulahouache,[16] S. Blusk,[16] K. Bukin,[16] E. Dambasuren,[16] R. Mountain,[16] H. Muramatsu,[16] R. Nandakumar,[16] T. Skwarnicki,[16] S. Stone,[16] J. C. Wang,[16] A. H. Mahmood,[17] S. E. Csorna,[18] I. Danko,[18] G. Bonvicini,[19] D. Cinabro,[19] M. Dubrovin,[19] S. McGee,[19] A. Bornheim,[20] E. Lipeles,[20] S. P. Pappas,[20] A. Shapiro,[20] W. M. Sun,[20] and A. J. Weinstein[20]

(CLEO Collaboration)

[1]*Carnegie Mellon University, Pittsburgh, Pennsylvania 15213, USA*
[2]*Cornell University, Ithaca, New York 14853, USA*
[3]*University of Florida, Gainesville, Florida 32611, USA*
[4]*University of Illinois, Urbana-Champaign, Illinois 61801, USA*
[5]*Carleton University, Ottawa, Ontario, Canada K1S 5B6 and the Institute of Particle Physics, Canada M5S 1A7*
[6]*University of Kansas, Lawrence, Kansas 66045, USA*
[7]*University of Minnesota, Minneapolis, Minnesota 55455, USA*
[8]*Northwestern University, Evanston, Illinois 60208, USA*
[9]*State University of New York at Albany, Albany, New York 12222, USA*
[10]*The Ohio State University, Columbus, Ohio 43210, USA*
[11]*University of Oklahoma, Norman, Oklahoma 73019, USA*
[12]*University of Pittsburgh, Pittsburgh, Pennsylvania 15260, USA*
[13]*Purdue University, West Lafayette, Indiana 47907, USA*
[14]*University of Rochester, Rochester, New York 14627, USA*
[15]*Southern Methodist University, Dallas, Texas 75275, USA*
[16]*Syracuse University, Syracuse, New York 13244, USA*
[17]*University of Texas–Pan American, Edinburg, Texas 78539, USA*
[18]*Vanderbilt University, Nashville, Tennessee 37235, USA*
[19]*Wayne State University, Detroit, Michigan 48202, USA*
[20]*California Institute of Technology, Pasadena, California 91125, USA*

(Received 20 February 2003; published 6 May 2003)

From electron-positron collision data collected with the CLEO detector operating at Cornell Electron Storage Ring near $\sqrt{s} = 10.6$ GeV, improved measurements of the branching fractions for τ decays into three explicitly identified hadrons and a neutrino are presented as $\mathcal{B}(\tau^- \to \pi^-\pi^+\pi^-\nu_\tau) = (9.13 \pm 0.05 \pm 0.46)\%$, $\mathcal{B}(\tau^- \to K^-\pi^+\pi^-\nu_\tau) = (3.84 \pm 0.14 \pm 0.38) \times 10^{-3}$, $\mathcal{B}(\tau^- \to K^-K^+\pi^-\nu_\tau) = (1.55 \pm 0.06 \pm 0.09) \times 10^{-3}$, and $\mathcal{B}(\tau^- \to K^-K^+K^-\nu_\tau) < 3.7 \times 10^{-5}$ at 90% C.L., where the uncertainties are statistical and systematic, respectively.

DOI: 10.1103/PhysRevLett.90.181802 PACS numbers: 13.35.Dx

For hadronic τ decays, final states with kaons provide a powerful probe of the strange sector of the weak charged current. In this Letter, we present the improved measurements of branching fractions for $\tau^- \to \pi^-\pi^+\pi^-\nu_\tau$, $K^-\pi^+\pi^-\nu_\tau$, and $K^-K^+\pi^-\nu_\tau$ decays, and an improved upper limit for the phase space suppressed and

Cabibbo-suppressed decay $\tau^- \to K^- K^+ K^- \nu_\tau$. (Charge conjugate decays are implied.) The decay mode $\tau^- \to K^- \pi^+ \pi^- \nu_\tau$ has a significant contribution to the overall strange spectral function which can provide a direct determination of the strange quark mass and, potentially, precision extraction of the Cabibbo-Kobayashi-Maskawa element V_{us} [1]. The decay $\tau^- \to K^- K^+ \pi^- \nu_\tau$ can proceed via both the vector and axial-vector currents [2] and, therefore, has a sensitivity to the Wess-Zumino anomaly [3].

The data used for this analysis were collected with the CLEO III detector [4] located at the symmetric e^+e^- Cornell Electron Storage Ring (CESR). The data sample consists of 3.26 fb^{-1} taken on or near the $\Upsilon(4S)$, corresponding to 2.97×10^6 $\tau^+\tau^-$ pairs. The CLEO III detector configuration features a new four-layer silicon strip vertex detector, a new wire drift chamber, and, most importantly for this analysis, a ring imaging Cherenkov (RICH) particle identification system. Particle trajectories, momenta, and charges are measured with the tracking system, which uses hits from both the silicon detector and drift chamber. The specific ionization, dE/dx, measured in the drift chamber's 16 inner axial and 31 outer stereo layers is sensitive to the traversing particle's mass. The RICH detector [5] surrounds the drift chamber and uses 1-cm-thick LiF radiators to generate Cherenkov photons from the incident charged particles. These photons then propagate through a 20-cm-thick expansion volume of gaseous nitrogen at atmospheric pressure and are detected by multiwire proportional chambers filled with a mixture of triethyleamine and CH_4 gases and localized by readout from 8-mm-square cathode pads located on a cylinder of $\sim$1 m radius. RICH particle identification is available over the central region of the detector, $|\cos\theta| < 0.83$, where θ is the polar angle with respect to the direction of the incident positron beam. A detailed description of the RICH performance can be found in Ref. [6]. The electromagnetic calorimeter surrounds the RICH detector and measures the energy, position, and lateral shape of showers induced by charged and neutral particles. It contains 7784 16-radiation-length-long CsI(Tl) crystals, arranged in a barrel section ($|\cos\theta| < 0.83$) and two end caps ($0.83 < |\cos\theta| < 0.95$). These components all operate inside a superconducting solenoid coil which creates a uniform magnetic field of 1.5 T. A muon detection system surrounds the solenoid coil with 1 m of iron absorber interspersed with Iarocci tube wire chambers operated in proportional mode.

We combine RICH and dE/dx information to determine if a track appears more consistent with a pion or kaon identity. The deviation of the measured dE/dx for any track from that expected under particle hypothesis i ($i = e, \mu, \pi, K, p$) at that momentum, in units of the expected Gaussian width of the distribution, is defined as δ_i. The dE/dx resolution is about 6% for hadrons. For each detected charged particle track, the RICH detector response is condensed into a χ^2_i-like variable for each particle hypothesis. The value of χ^2_i is derived from the number N^i_γ of detected Cherenkov photons and their locations relative to the Cherenkov cone expected for a particle with that momentum and mass. Pions and kaons are distinguished from one another with the combined RICH-dE/dx variable $\Delta\chi^2 = \chi^2_\pi - \chi^2_K + \delta^2_\pi - \delta^2_K$. We identify a track as a pion (kaon) if $|\cos\theta| < 0.83$, $N^\pi_\gamma(N^K_\gamma) \geq 3$, $\Delta\chi^2 < (>)0$ and apply these criteria to three-prong-side tracks. For the pion in $\tau^- \to K^- K^+ \pi^- \nu_\tau$, $|\delta_\pi| < 3.0$ alone is used, yielding $\sim$10% higher efficiency from a looser criterion as well as the region outside the RICH acceptance, $0.83 < |\cos\theta| < 0.93$. The consequently higher K-fakes-π rate is unimportant for this mode due to the dearth of three-kaon events.

We take advantage of the copious cascade decays $D^{*+} \to D^0\pi^+$ with $D^0 \to K^-\pi^+$, in which the charged kaon and pion can be tagged kinematically without reference to RICH or dE/dx information, to measure the probability for pions and kaons to be correctly or incorrectly identified. This method measures the area above background of the $K^-\pi^+$ mass peak with and without the particle identification criteria to determine the efficiency and fake rates for both pions and kaons. We find that the efficiency for pion and kaon identification ranges from 80%–95% over most of the momentum range of interest for this analysis (0.5–3 GeV/c) and that the probability for a pion to fake a kaon or vice versa ranges from 1%–2% for momentum values of 0.5–2 GeV/c and rises to about 10%–15% for momenta around 3 GeV/c, as shown in Fig. 1.

Events are required to have four well-measured charged particles in a one-versus-three topology (the two hemispheres being defined by the event thrust axis) and zero net charge. We use one-prong τ leptonic (e/μ) or hadronic decays (ρ/π) to "tag" the event. An electron tag requires the lone track to have $\delta_e > -2$ and E/p, the ratio of energy deposited in the calorimeter to track momentum, to satisfy $0.85 < E/p < 1.1$. These criteria attain $\sim$95% efficiency and a pion-faking-electron probability less than 1%. A muon tag must have the lone track penetrate at least three (if $p < 2$ GeV/c) or five (if $p > 2$ GeV/c) absorption lengths of material, which achieves 80%–90% efficiency and a few percent pion-faking-muon probability for $p > 1$ GeV/c.

If the tagside track is not identified as an electron or a muon, tagside calorimeter showers are then examined. If the invariant mass of the lone track and showers in the tagging hemisphere not matched to that track is below 0.5 GeV/c^2, the event is classified as a π tag. To establish a $\rho^-(\to \pi^-\pi^0)$ tag, we require a $\pi^0 \to \gamma\gamma$ candidate on the one-prong side. For photon candidates, we select showers which do not match the projection of any charged-track trajectories into the calorimeter, have

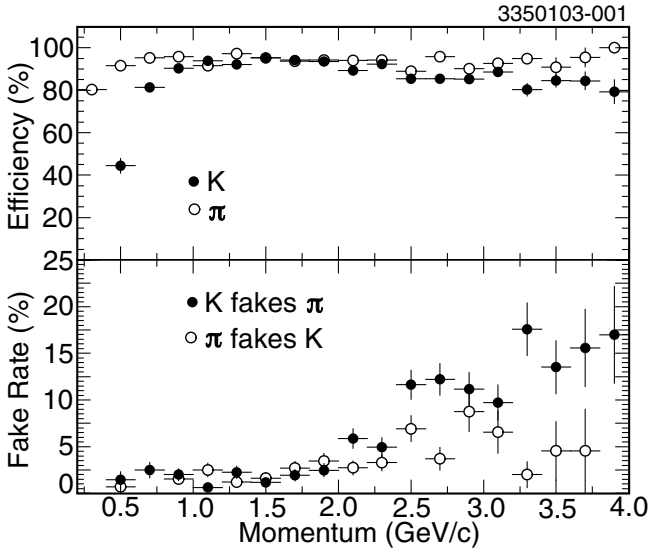

FIG. 1. Kaon (solid circles) and pion (open circles) identification efficiencies (top) and fake rates (bottom) as a function of their momenta for tracks already within $|\cos\theta| < 0.83$ as determined from $D^0 \to K^-\pi^+$ decays. Error bars are statistical only.

energies exceeding 30 (50) MeV in the barrel (end caps), and have compact lateral profiles consistent with those expected from electromagnetic showers. At least one photon from any π^0 candidate decay must be located in the barrel. We take the most energetic $\gamma\gamma$ pair which has invariant mass within $(-3.0, 2.5)$ standard deviations of m_{π^0}(typically a window $\sim$30 MeV/c^2 wide). After kinematically constraining the $\gamma\gamma$ pair to m_{π^0}, the invariant mass of this fitted π^0 candidate and the associated charged track, assigned the pion mass, is required to be consistent with the ρ mass: $0.5 < m(\pi^-\pi^0) < 1.0$ GeV/c^2.

To suppress backgrounds with one or more neutral particles, we do not allow any shower in the event unassociated with a charged track or a π^0 participating in ρ tagging with energy exceeding 100 MeV. After the event selection, the backgrounds with extra neutrals contribute 4.1%, 2.1%, and 2.6% of the total observed events for the channels with zero, one, and two kaons, respectively. In order to reject two-photon backgrounds (characterized by the missing momentum along the beam direction and low visible energy), the missing momentum must point into the CLEO detector ($|\cos\theta_{\rm miss}| < 0.95$) and the visible energy must exceed 20% of the e^+e^- center-of-mass energy. For all modes, we further demand that the three-prong mass, calculated using mass assignments determined from particle identification, lie below the τ mass. For the decay $\tau^- \to K^-\pi^+\pi^-\nu_\tau$, a veto of K^0_S candidates with $K^0_S \to \pi^+\pi^-$ within 10 MeV/c^2 of the K^0_S nominal mass and a production vertex more than 1 cm from the primary interaction point is applied. Any K^0_s content in both modes with two or more pions is treated as background, not signal.

Efficiencies and the remaining backgrounds are evaluated with Monte Carlo (MC) events from the KORALB [7] (τ-pairs) and JETSET [8] ($q\bar{q} \to$ hadrons) generators passed through the GEANT-based [9] CLEO detector simulation. Any MC event which has a tagside particle which is truly $e^\pm$, $\mu^\pm$, $\pi^\pm$, $K^\pm$, or $\rho^\pm$ is considered signal for purposes of efficiency; other tags are considered background even if the three-prong side is a signal decay mode. For $\tau^- \to K^-K^+K^-\nu_\tau$ decay, we generate signal MC samples according to phase space. The particle identification simulation models the general features of the efficiency and fake rates reasonably well (at the few percent level). We correct the Monte Carlo efficiencies and fake rates by hand, using momentum-dependent scale factors derived from measured and MC particle identification rates.

The corrected efficiencies for events in which one τ decays into a tag mode and the other into the relevant signal mode (integrated over all tag modes, which constitute about 72.4% of all τ decays), observed numbers of events in the data, and the expected numbers of τ and $q\bar{q}$ background events are given in Table I. There are substantial signals evident in all but the three-kaon mode. The largest backgrounds come from τ decays to three charged hadrons with a single misidentification of a pion or kaon. Many such events are eliminated by the restriction of three-prong mass to be below the τ mass. Each decay in Table I contributes the dominant background for the channel below it due to the particle misidentification. For the $\tau^- \to K^-K^+K^-\nu_\tau$ decay, the τ background is not taken from the Monte Carlo sample, but rather the measured π-fakes-K rate is applied to the $K^-K^+\pi^-$ events in the data (many of which subsequently fail the three-prong mass restriction).

In Fig. 2, we show the three-hadron masses for the four modes considered here along with the results from the overlaid MC simulation. The two-particle substructure is presented in Fig. 3. Good agreement between the data and MC is observed [10,11]. The $\tau^- \to K^-K^+\pi^-\nu_\tau$ mode can be used to measure the contribution from the Wess-Zumino anomaly, offering an alternative channel to $\tau^- \to \eta\pi^-\pi^0\nu_\tau$. A quantitative estimate requires

TABLE I. Candidate event yields for the data, estimated τ and $q\bar{q}$ background event totals, and overall efficiencies ϵ for τ three-prong decays.

Mode	Data	τ bgd	$q\bar{q}$ bgd	ϵ (%)
$\pi^-\pi^+\pi^-\nu_\tau$	43 543	3207 ± 57	152 ± 12	10.27 ± 0.08
$K^-\pi^+\pi^-\nu_\tau$	3454	1475 ± 38	57 ± 8	11.63 ± 0.12
$K^-K^+\pi^-\nu_\tau$	932	86 ± 9	19 ± 4	12.48 ± 0.11
$K^-K^+K^-\nu_\tau$	12	4 ± 2	0.4 ± 0.6	9.43 ± 0.10

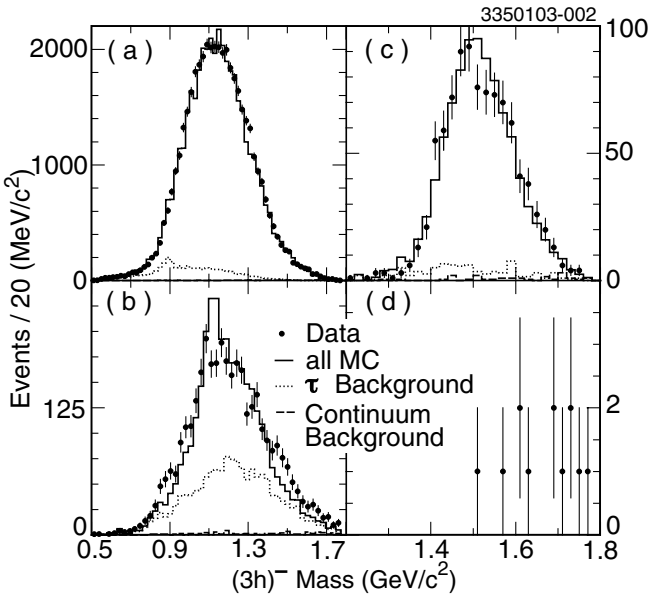

FIG. 2. Three-hadron masses from data (solid circles) and MC, τ-pair background (short dashes), $q\bar{q}$ background (long dashes), sum of background and signal (solid lines), for (a) $\tau^- \to \pi^-\pi^+\pi^-\nu_\tau$, (b) $\tau^- \to K^-\pi^+\pi^-\nu_\tau$, (c) $\tau^- \to K^-K^+\pi^-\nu_\tau$, and (d) $\tau^- \to K^-K^+K^-\nu_\tau$.

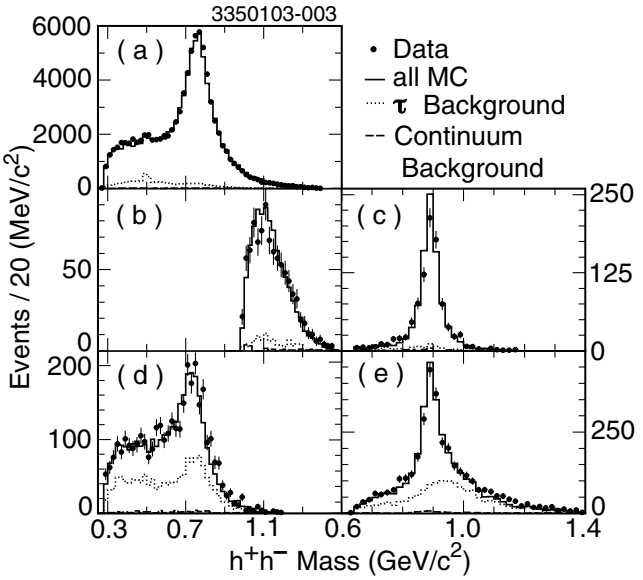

FIG. 3. Mass distributions for two oppositely charged hadrons showing the data (solid circles) and MC [τ-pair background (short dashes), $q\bar{q}$ background (long dashes), sum of background and signal (solid lines)] for (a) $\tau^- \to \pi^-\pi^+\pi^-\nu_\tau$ (two entries per event), (b),(c) $\tau^- \to K^-K^+\pi^-\nu_\tau$, ($K^+K^-$ and $K^+\pi^-$ masses, respectively), and (d),(e) $\tau^- \to K^-\pi^+\pi^-\nu_\tau$ ($\pi^+\pi^-$ and $K^-\pi^+$ masses, respectively).

determination of the structure functions [2], for which a substantially larger data sample would be needed.

Most sources of systematic uncertainty affect the four modes similarly. MC statistics for signal events add 1% uncertainty. The uncertainty in the number of τ-pair events produced, and therefore in the normalization of the branching fractions, derives from the uncertainty of luminosity [12] (2%) and τ-pair cross section (2%) [7]. Studies comparing track-finding efficiencies in the MC simulation to data result in a 0.5% per track uncertainty, added linearly to become 2% for the entire event. Several effects are probed individually by tightening and/or relaxing an event selection criterion, recalculating the branching fractions, and assigning an uncertainty in how well the MC models reality based on the changes induced: allowing for an extraneously reconstructed track in signal events adds 2% uncertainty, one systematic error arising from the assumed absence of two-photon physics background is 0.5% which can be tested by imposing a harsh net transverse momentum of the three-prong side requirement of 3 GeV/c, uncertainty due to the background levels from decay modes with extra neutrals allowed in is estimated by relaxing the veto energy on extra calorimeter showers to as high as 250 MeV and found to be 1%, and variations of the remaining non-particle-identification selection criteria contribute an error of 1%. Uncertainty in τ branching fractions results in 1% error due to changes in τ backgrounds. The efficiencies of particle identification were studied exhaustively for variations with time (0.5%) or charged-track multiplicity (0.5%), bias of the efficiency-measuring technique (0.5%), the data/MC efficiency correction procedure (0.4%), and statistics of the D^* data samples (0.3%), which all sum in quadrature to 1% per pion or kaon, which then are added linearly for the event as a whole to 3% overall. When the branching fractions are broken out by individual tags, consistent results are obtained, verifying both the modeling of tag efficiencies and the lack of unexpected non-τ backgrounds which sometimes show up in the nonleptonic tags. Together these errors sum in quadrature to 5%, which applies to the branching fractions of all four modes.

Other systematics vary from mode to mode, which will be referred to in the order in which they appear in Table I. To estimate uncertainties from $q\bar{q}$ backgrounds, we compare event totals above the τ mass between the data and $q\bar{q}$ MC and assign an additional $\sim$50% (relative) uncertainty from the observed differences. This results in uncertainties of 0.2%, 2%, 1%, and 3% for the four modes, respectively. An overall scale uncertainty in the fake rate per pion or kaon of 0.25% (absolute) is estimated by comparing measured results to those predicted by the RICH simulation, cross-checking with MC for possible bias in the fake-rate measurement technique, examining the rate of the forbidden $\tau^- \to K^+\pi^-\pi^-\nu_\tau$ (which is dominated by $\tau^- \to \pi^+\pi^-\pi^-\nu_\tau$ with a pion faking a kaon), and estimating the error from the momentum-reweighting correction procedure. This fake-rate uncertainty propagates to the branching fractions differently because of different levels of feed down: 0.1%, 9%, 2%, and 12%, respectively. The $K^-K^+\pi^-$ mode substructure

is not well understood, and variations in the possibilities result in a 2% uncertainty in the efficiency. The three-kaon mode substructure is completely unknown and assumed to occur via phase space with no assigned error. The remaining modes appear to be adequately described by the models used. Adding these contributions together in quadrature with the common sources results in total relative systematic uncertainties of 5%, 10%, 6%, and 14%, respectively.

For all decay modes, the yields are obtained from the numbers of the observed events with the backgrounds subtracted; the measured branching fractions (with K_S^0 excluded from the modes with two or more pions) are

$$\mathcal{B}(\tau^- \to \pi^-\pi^+\pi^-\nu_\tau) = (9.13 \pm 0.05 \pm 0.46)\%,$$
$$\mathcal{B}(\tau^- \to K^-\pi^+\pi^-\nu_\tau) = (3.84 \pm 0.14 \pm 00.38) \times 10^{-3},$$
$$\mathcal{B}(\tau^- \to K^-K^+\pi^-\nu_\tau) = (1.55 \pm 0.06 \pm 0.09) \times 10^{-3},$$
$$\mathcal{B}(\tau^- \to K^-K^+K^-\nu_\tau) < 3.7 \times 10^{-5} \quad \text{at 90\% CL}..$$

The errors are statistical and systematic, respectively. For the decay $\tau^- \to K^-K^+K^-\nu_\tau$, the upper limit is obtained according to the procedure described in the Particle Data Group (PDG) [13] with both statistical and systematic errors taken into account. This represents the first direct measurement of $\mathcal{B}(\tau^- \to \pi^-\pi^+\pi^-\nu_\tau)$ with three pions explicitly identified, and our result is in good agreement with the PDG fitted value derived from the PDG constrained fit to the measurements of $\tau^- \to (3h)^-\nu_\tau$ decays with and without identified charged kaons [13]. The measurement of $\mathcal{B}(\tau^- \to K^-K^+\pi^-\nu_\tau)$ is consistent with the previous value [13] and improves upon the precision previously attained by a factor of 2. Our result $\mathcal{B}(\tau^- \to K^-\pi^+\pi^-\nu_\tau)$ is more precise than and consistent with both the CLEO [14] and OPAL [15] results, while it is larger than the ALEPH [16] value by nearly 3 standard deviations. The upper limit for the Cabibbo-suppressed decay $\tau^- \to K^-K^+K^-\nu_\tau$ has been improved over the PDG value [13] by a factor of 5. Taken together, these measurements significantly enhance our understanding of the kaon content of three-prong τ decays.

We gratefully acknowledge the effort of the CESR staff in providing us with excellent luminosity and running conditions. This work was supported by the National Science Foundation, the U.S. Department of Energy, the Research Corporation, and the Texas Advanced Research Program.

[1] ALEPH Collaboration, R. Barate *et al.*, Eur. Phys. J. C **11**, 599 (1999); S. Chen *et al.*, Eur. Phys. J. C **22**, 31 (2001); A. Pich and J. Prades, J. High Energy Phys. **10**, 004 (1999); S. Narison, Phys. Lett. B **466**, 345 (1999).
[2] R. Decker *et al.*, Phys. Rev. D **47**, 4012 (1993).
[3] J. Wess and B. Zumino, Phys. Lett. **37B**, 95 (1971).
[4] CLEO Collaboration, Y. Kubota *et al.*, Nucl. Instrum. Methods Phys. Res., Sect. A **320**, 66 (1992); T. Hill, Nucl. Instrum. Methods Phys. Res., Sect. A **418**, 32 (1998); D. Peterson *et al.*, Nucl. Instrum. Methods Phys. Res., Sect. A **478**, 142 (2002).
[5] T. Coan, Nucl. Instrum. Methods Phys. Res., Sect. A **379**, 448 (1996).
[6] M. Artuso *et al.*, hep-ex/0209009 [in Proceedings of the Fourth Workshop on RICH Detectors, Pylos, Greece, 2002 (to be published)].
[7] S. Jadach and Z. Was, Comput. Phys. Commun. **36**, 191 (1985); **64**, 267 (1991); **76**, 361 (1993); **85**, 453 (1995); R. Decker *et al.*, Z. Phys. C **58**, 445 (1993); M. Finkemeier and E. Mirkes, Z. Phys. C **69**, 243 (1996). The KORALB package [7] does not include higher order contributions to the τ production cross section. We take the difference (2%) between the cross sections from KORALB and its successor $\mathcal{KK}$ MC with higher order corrections as the systematics due to the τ pair cross section. For the $\mathcal{KK}$ MC, see S. Jadach, B. F. L. Ward and Z. Was, Comput. Phys. Commun. **130**, 260 (2000).
[8] T. Sjostrand, CERN Report No. CERN-TH-6488-92 (unpublished).
[9] R. Brun *et al.*, GEANT3.14, CERN Report No. CERN DD/EE/84-1 (unpublished).
[10] For $\tau^- \to K^-K^+\pi^-\nu_\tau$ decay, we obtain the good data-MC agreement of mass distributions shown solely by tuning the parameters of the form factor. We increase the ρ' contribution and suppress the K^{*0} component on the low mass side compared to the default model, switching off the ρ'' contribution and renormalizing it.
[11] All CLEO results on the branching fractions and resonance contents of the decays $\tau^- \to (3\pi)^-\nu_\tau$ and $\tau^- \to K^-\pi^+\pi^-\nu_\tau$ have been implemented in the Monte Carlo program. For experimental results, see D. M. Asner *et al.*, Phys. Rev. D **61**, 012002 (2000) and D. M. Asner *et al.*, Phys. Rev. D **62**, 072006 (2000); see also A. Weinstein, hep-ex/0210058 [in Proceedings of Tau'02, Santa Cruz, CA, 2002 (to be published)].
[12] CLEO Collaboration, G. Crawford *et al.*, Nucl. Instrum. Methods Phys. Res., Sect. A **345**, 429 (1994).
[13] Particle Data Group, K. Hagiwara *et al.*, Phys. Rev. D **66**, 010001 (2002).
[14] CLEO Collaboration, S. Richichi *et al.*, Phys. Rev. D **60**, 112002 (1999).
[15] OPAL Collaboration, G. Abbiendi *et al.*, Eur. Phys. J. C **13**, 197 (2000).
[16] ALEPH Collaboration, R. Barate *et al.*, Eur. Phys. J. C **1**, 65 (1998).